LANGMUIR

pubs.acs.org/Langmuir
Article

Thermal Vapor Deposition of a Hydrophobic and Gas-Permeable Membrane on Zirconium Phosphate Cation Exchanger: An Oral Sorbent for the Urea Removal of Kidney Failure

Yihan Song, Sang-Ho Ye, Stephen R. Ash,* and Lei Li*

Cite This: *Langmuir* 2024, 40, 16502−16510
Read Online

ABSTRACT: An oral sorbent with high capacity for NH_4^+ is desirable in lowering the blood urea level and mitigating the dialysis burden for end-stage kidney disease (ESKD) patients. Zirconium phosphate (ZrP) is an amorphous cation ion exchanger with high NH_4^+ binding capacity as a sorbent material, but its selectivity to remove NH_4^+ is limited in the presence of other competing ions in water solution. We previously have developed a gas-permeable and hydrophobic perfluorocarbon coating on ZrP, which improves ZrP's NH_4^+ selectivity. However, the coating preparation procedure, a wet chemistry approach, is complicated and time-consuming, and more importantly, the large amount of usage of acetone poses a concern for the application of ZrP as an oral sorbent. In this study, we developed a solventless coating protocol that effectively coats ZrP with tetraethyl orthosilicate (TEOS) and 1*H*,1*H*,2*H*,2*H*-perfluorooctyltriethoxysilane (FOTS) via thermal vapor deposition (TVD) in a simplified manner. X-ray photoelectron spectroscopy (XPS) and contact angle measurements verify the two coatings are successfully deposited on the ZrP surface, and the coating condition was optimized based on an *in vitro* static binding study. The dynamic binding study of competing ions on Na-loaded ZrP with TVD coatings yields a maximum NH_4^+ removal (~3.2 mequiv/g), which can be improved to ~4.7 mequiv/g if H-loaded ZrP under the same coating condition is used in basic stock solutions. More importantly, both materials barely remove Ca^{2+} and show excellent acid resistance. The significant improvement in the NH_4^+ binding capacity and selectivity reported here establishes a highly promising surface modification approach to optimize oral sorbents for ESKD patients.

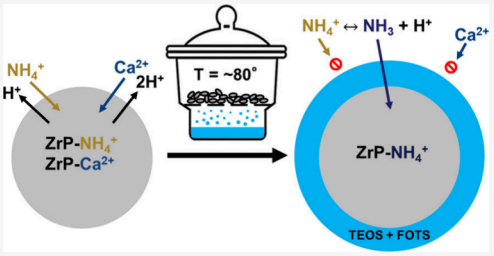

1. INTRODUCTION

Chronic kidney disease (CKD) is a rapidly growing global public health burden, affecting more than 10% of the worldwide population.[1,2] Approximately 786,000 people in the United States are currently living with end-stage kidney disease (ESKD), which is defined as the final stage of CKD treated with dialysis or a kidney transplant.[3] Kidney transplantation is considered as the optimal therapeutic approach for ESKD, but the supply of available kidneys cannot satisfy the current demand, along with the downsides of high graft failure rate and the ineligibility of many patients for this treatment.[4] Hence, the majority of patients with ESKD rely on hemodialysis or peritoneal dialysis as a substitute for kidney function. However, patients undergoing hemodialysis are constrained by the need to visit the clinic three times a week, enduring up to 4 h per session, which restricts their freedom and autonomy.[5] Unlike a healthy kidney that consistently maintains homeostasis, the intermittent nature of hemodialysis treatment results in the buildup of uremic waste solute, water, and electrolytes such as Na^+, K^+, and PO_4^{3-}, which are associated with conditions such as hypertension and cardiovascular disease.[4,5] Peritoneal dialysis offers more continuous in-home treatment.[6,7] However, its overall toxin removal efficiency is lower than hemodialysis, and the rapid functional decline of the peritoneal membrane in high-concentration glucose limits the technique's lifetime.[6,7] Thus, patients typically transition to hemodialysis as their treatment option after an average of 3.7 years.[8] The conventional dialysis treatment results in considerable treatment burden, dietary restrictions, and poor clinical outcomes.[4,5,7,9,10] Therefore, an improved ESKD treatment approach could benefit both the patient and clinician.

A wearable or highly portable artificial kidney (WAK or PAK) with light weight and high toxin clearance away from the clinic could improve patient life quality by increasing their mobility, freedom, and ability to engage in social and economic life.[4,11] The "REDY sorbent system" was a PAK used in home dialysis from 1973 to 1994.[12] Such devices incorporate zirconium phosphate (ZrP, a nonselective cation exchanger) sorbent into a dialysis circuit to continuously regenerate dialysate through the adsorption of ammonium ions resulting

Received: May 17, 2024
Revised: July 6, 2024
Accepted: July 15, 2024
Published: July 23, 2024

https://doi.org/10.1021/acs.langmuir.4c01877
Langmuir 2024, 40, 16502−16510

from enzymatic breakdown of urea.[4,12] However, ZrP's nonselectivity in the presence of other ions, including calcium, magnesium, and potassium, limits its binding capacity to 0.96 mequiv of NH_4^+/g of ZrP and lowers the level of these ions, which need to be infused back into the dialysate.[4] The adsorbed ions are exchanged for hydrogen and sodium ions, and sodium release is a concern, as higher sodium concentration in the dialysate is associated with hypertension.[13] Minimization of Ca^{2+} removal and Na^+ release in the dialysate has complicated the WAK or PAK and increased its size and weight.[13,14]

An oral sorbent could effectively bind and remove small and charged uremic toxins in the gut (SCUT: K^+, H^+, phosphate, NH_4^+ from urea), and thus dialysis therapy for ESKD could be directed principally at removal of organic and protein-bound toxins.[15] A charcoal column is all that would be needed to accomplish effective regeneration of the dialysate, thus leading to the greatly simplified construction of a WAK or PAK.[15] For decades oral sorbents such as anion exchangers have been used to decrease serum phosphate in patients with CKD and ESKD.[16] Zirconium oxide loaded with hydroxide (ZO-OH) is well tolerated in animal studies and effective in binding phosphate in the gut.[15] Zirconium cyclosilicate (ZS), a monovalent-selective cation exchanger, is highly effective for removal of potassium.[17,18] However, there is no oral sorbent for effectively removing NH_4^+ or urea from the gut. About 25% of the urea generated by the liver in normal patients diffuses into the small bowel lumen daily. This urea is catalyzed to ammonium ion (NH_4^+) and bicarbonate by urease, and the products return to the liver, which resynthesizes the urea. In patients with CKD and elevated blood urea nitrogen (BUN) levels, the transfer of urea to the gut increases in proportion to the BUN. Thus, an effective oral sorbent for binding NH_4^+ in the gut should lower the BUN level in CKD patients. The above-mentioned ZrP is an excellent NH_4^+ binder, but the presence of competing ions limits binding capacity.[4] Several urea removal strategies, including enzymatic hydrolysis, electrochemical decomposition, and urea sorbents, have been studied for WAK, but these approaches have toxic side effects or limited removal capacity.[4]

Our previous works demonstrated that a nonselective cation exchanger, ZrP, could be coated with a gas-permeable and hydrophobic membrane to improve its binding capacity for NH_4^+ and selectivity in the presence of other ions.[5,12] The hydrophobic coating acts as a barrier to ions in water solution interacting with the cation exchanger. NH_4^+ is in equilibrium with NH_3 in any solution. The coating's gas permeability allows gaseous NH_3 to transfer to the H-loaded exchanger. NH_3 could pass through the membrane and bind with H^+ to form NH_4^+, and thus it could be trapped within the capsule. However, the procedure for creating these membranes within a liquid environment is complex and consumes large amounts of acetone, which is a concern when it comes to oral sorbents.

Vapor-phase deposition is an alternative to this wet chemistry coating method, in which silanes can be coated on a solid surface from precursors vaporized under an elevated temperature or reduced pressure. Previous works[19−23] have demonstrated that a monolayer or multilayers could form in the vapor phase depending on the reaction conditions, the chemistry of the silane molecule, and the surface structure. In addition, surface silanization within the vapor phase has been found promising in many applications, such as superhydrophobicity,[24,25] anticorrosion,[26,27] antistiction,[28,29] blood-contacting medical devices,[30,31] and biosensors.[32−34] In this work, we hypothesized that the hydrophobic and gas-permeable membrane can be grafted onto ZrP in the vapor phase, which has been achieved by a simple solventless thermal vapor deposition (TVD) process. *In vitro* competing ion tests indicate that coated ZrP has significantly improved NH_4^+ binding capacity and selectivity, suggesting that a solventless procedure, such as vapor-phase deposition, is more promising for developing oral sorbents for ESKD patients.

2. EXPERIMENTAL SECTION

2.1. Materials. Amorphous ZrP loaded with sodium or hydrogen in granular form was provided by HemoCleanse Technologies LLC (Lafayette, IN, USA). Tetraethyl orthosilicate (TEOS)-coated ZrP was prepared following a wet chemistry protocol reported previously.[5,12] TEOS, 1*H*,1*H*,2*H*,2*H*-perfluorooctyltriethoxysilane (FOTS), HEPES sodium salt, acetone, calcium chloride, and ammonium chloride were purchased from Sigma-Aldrich (St. Louis, MO, USA). Hydrogen chloride was obtained from Fisher Scientific (Waltham, MA, USA). Colorimetric testing kits for measurement of total nitrogen and calcium were purchased from Teco Diagnostics (Anaheim, CA, USA). Cuvettes of 4.5 and 3 mL were purchased from Fisher Scientific (Waltham, MA, USA) and Cole-Parmer (Vernon Hills, IL, USA), respectively.

2.2. TVD Coating Preparation. A simple TVD process was utilized to expose ZrP particles to the vapor of a coating precursor at elevated temperature (~80 °C) for different durations. Using the TVD setup shown in Figure 1, 1 g of ZrP particles was placed on

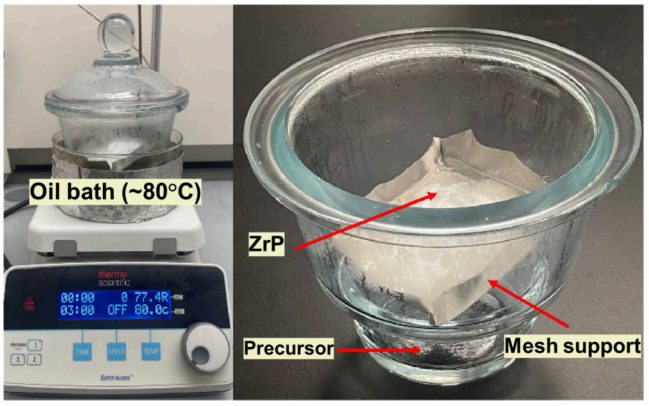

Figure 1. TVD setup showing the treatment of ZrP with TEOS or FOTS.

porous stainless-steel mesh in a closed chamber with an open vessel holding ~1 mL of FOTS or ~5 mL of TEOS for a duration ranging from 1 to 48 h at 80 °C. Coated ZrP materials are named as coating precursor (T/F) followed by TVD duration (1−48 h). For example, T24hF12h refers to ZrP coated by TEOS for 24 h and then by FOTS for 12 h, while TF12h indicates the ZrP material coated by solution-based TEOS and then vapor-phase FOTS for 12 h.

2.3. Acid Exposure Study. A HCl solution (pH = 2) was prepared, and 100 mg coated ZrP was added into a 20 mL solution in 50 mL centrifuge tubes.[12] Capped tubes were placed upright for 3 h. The HCl solution was carefully removed from the tubes, and then, the coated ZrP was washed with DI water three times. The washed samples were air-dried in ambient conditions.

2.4. Characterization. *XPS.* The atomic surface composition of uncoated and coated ZrP materials was determined using XPS at the University of Washington's Molecular Analysis Facility. Each sample was pressed flat onto a piece of double-sided Scotch tape that was adhered to a clean silicon wafer. Three spots on each sample were chosen for analysis. XPS spectra were taken on a Surface Science Instruments S-Probe spectrometer. This instrument has a mono-

https://doi.org/10.1021/acs.langmuir.4c01877
Langmuir 2024, 40, 16502−16510

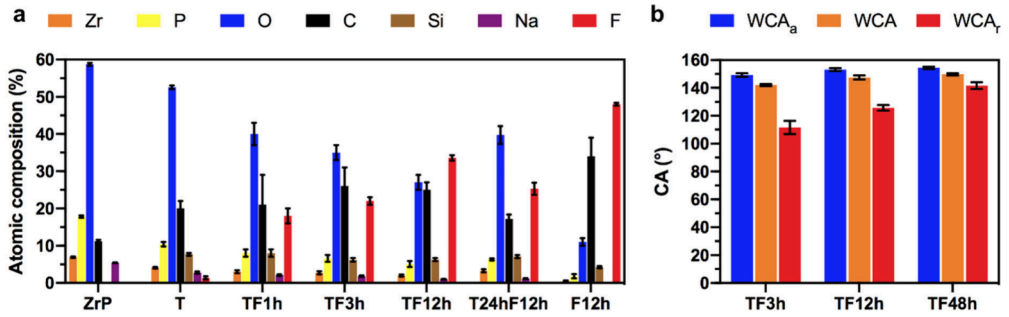

Figure 2. Atomic surface composition (a) and water contact angle (b) of ZrP with different coatings. "ZrP" is an uncoated material as the control. "T" refers to ZrP coated with TEOS in liquid phase, while "TF1h", "TF3h", and "TF12h" are ZrPs that were coated with TEOS in liquid phase followed by FOTS in vapor phase for 1, 3, and 12 h, respectively. "T24hF12h" was ZrP coated by TEOS vapor in 24 h exposure followed by FOTS vapor in 12 h exposure. "F12h" represents that ZrP was coated with FOTS only in vapor phase for 12 h.

chromatized Al X-ray source and a low-energy electron flood gun for charge neutralization. X-ray spot size for these acquisitions was 800 × 800 μm or 200 × 200 μm. All samples were run as insulators. Pressure in the analytical chamber during spectral acquisition was about 5 × 10^{-9} Torr. Pass energy for survey spectra was 150 eV. A detailed scan was run for Zr, F, P, Si, and Na to improve quantification. Data analysis was carried out using the Service Physics Hawk Analysis 7 program (Service Physics, Bend, OR, USA).

SEM. SEM images of uncoated and coated ZrP materials were taken using a Zeiss SIGMA VP scanning electron microscope (Nanoscale Fabrication & Characterization Facility at the University of Pittsburgh) with the electron source of a Schottky thermal field emitter under high vacuum. The accelerating voltage utilized was 3 kV.

Contact Angle. The static and dynamic water contact angles of ZrP materials were measured using a VCA Optima XE (AST Production Inc., Billerica, MA, USA) system at room temperature and 48% humidity. Samples of ∼50 mg of each material were pressed into pellets using a pellet die. Static water contact angle was measured by the VCA software after placing a 1 or 2 μL droplet on the sample surface. The advancing water contact angle (WCA_a) was measured by recording the continuous addition of water to a sessile drop (2 μL) for 5−8 s. Receding water contact angle (WCA_r) measurements were taken by withdrawing water from the droplet for 8 s. The moment when the contact angle is maximum (minimum) is taken as the advancing (receding) contact angle: WCA_a is the moment right before the droplet width increases, and WCA_r is the moment right before the droplet width decreases.

Binding Study. In vitro competing ion studies were carried out to determine NH_4^+ binding capacity and selectivity of uncoated and coated ZrP materials in the presence of a competing ion.[12] A testing solution containing 15 mM NH_4^+, 15 mM Ca^{2+}, and 20 mM sodium based HEPES was prepared for this study. A 5 mL amount of testing solution and 50 mg of each ZrP material were placed into a 24 mL test tube, which was capped and placed on a shaker plate at 270 rpm. Each test tube was tested for the concentrations of NH_4^+ and Ca^{2+} via colorimetric analysis over a period of 24 h.

To mimic small intestine physiological conditions for ESKD patients, *in vitro* binding studies with continuously replacing the stock solution were conducted.[5] A 5 mL amount of solution comprised 14 mM NH_4^+ and 12 mM Ca^{2+}, and 50 mg of each ZrP material was placed into a 24 mL test tube, which was capped and placed on a shaker plate at 270 rpm. The solution in each test tube was replaced every 20 min for 5 h, and the three 20 min samples from each hour were combined to determine the concentrations of NH_4^+ and Ca^{2+} via colorimetric analysis.

Single ion binding studies were performed to determine the NH_4^+ equilibrium adsorption curves for uncoated and coated ZrP materials. Stock solutions were prepared to cover a range of concentrations: 15, 25, 35, 45, and 75 mM NH_4^+. HEPES (20 mM) was added to each solution to buffer the pH (∼8.3) during the binding studies. A 5 mL amount of solution and 50 mg of each ZrP material were placed into a 24 mL test tube, which was capped and placed on a shaker plate at 270 rpm. After 24 h, test tubes were removed from the shaker plate, and the NH_4^+ concentration of each tube was measured via colorimetric analysis.

Colorimetric Analysis. NH_4^+/NH_3 and Ca^{2+} colorimetric testing kits obtained from Teco Diagnostics were used to quantify NH_4^+ and Ca^{2+} concentrations in stock solutions.[12] Color development assays were prepared by following the instructions provided with each kit. NH_4^+ and Ca^{2+} concentrations were quantified using a Genesys S10 UV−vis monochromator in Dr. Haitao Liu's Laboratory at the University of Pittsburgh. The wavelength of the monochromator was set to 570 nm for Ca^{2+} and 630 nm for NH_4^+ measurements. NH_4^+ and Ca^{2+} by sorbent materials was calculated from the depleted amount of NH_4^+ or Ca^{2+} in stock solutions.

3. RESULTS AND DISCUSSION

3.1. Characteristics of Coated Na-Loaded ZrP. XPS surface analysis results shown in Figure 2a include the atomic composition of uncoated and coated ZrP with different TVD conditions. The emergence of Si and F for coated materials with decreased Zr and P surface concentrations indicates TEOS and FOTS were successfully deposited on the ZrP surface. XPS has a takeoff angle of 90° and quantifies atoms to a depth of ∼10 nm beneath the surface. Thus, the coating thickness of TEOS plus FOTS is less than 10 nm, as indicated by the detection of some Zr and P. With increasing the TVD duration from 1 h to 12 h for FOTS coating, F composition increases from ∼18% to ∼34%. This is because longer TVD time allows more FOTS molecules to bombard and bond to the surface and thus guarantees more complete coating coverage to the ZrP surface. The dependence of surface coverage on reaction duration agrees with previous studies.[22,35] T24hF12h has the TEOS coating step performed in TVD as well, which shows a lower composition of C (∼17%) and F (∼25%) but higher composition of O (40%) by comparison to TF12h (C ≈ 25%, F ≈ 34%, and O ≈ 27%,). This could be attributed to adsorption of TVD reaction byproducts (e.g., H_2O and C_2H_5OH) onto the ZrP surface because our TVD is not followed by a washing step. F12h is a ZrP material coated with FOTS only, which has an atomic surface composition nearly equivalent to the theoretical composition of FOTS (F = 52%, C = 32%, Si = 4%, O = 12%). The Zr and P compositions on this material are negligible (<2%), indicating FOTS coating alone on ZrP gives rise to a thickness of at least 10 nm.

The results of the WCA measurement on coated ZrP materials are shown in Figure 2b. TF3h, TF12h, and TF48h have a WCA of ∼142°, ∼147°, and 149°, respectively, indicating the successful deposition of FOTS on the ZrP

https://doi.org/10.1021/acs.langmuir.4c01877
Langmuir 2024, 40, 16502−16510

surface, and all coated materials are very hydrophobic. The advancing (WCA_a) and receding (WCA_r) contact angles of these materials were also measured. The WCA_a is ~151° for all 3 materials, but WCA_r becomes higher for ZrP coated with longer TVD duration, leading to smaller difference in contact angle hysteresis ($WCA_a - WCA_r$: ~38° for TF3h and ~13° for TF48h). This can be explained by the fact that a shorter TVD duration results in incomplete surface coverage of the FOTS coating, and those defects play an important role in WCA_r measurements.

SEM images in Figure 3 reveal the surface morphologies of ZrP particles with different coatings. Uncoated ZrP in Figure 3a shows a porous surface texture, and its average particle size is ~30 μm. Coated ZrP materials (T and TF12h) in Figure 3b,d have similar surface appearance to uncoated ZrP without considerable particle aggregation. The F12h without TEOS coating in Figure 3c shows some degree of aggregation, and the FOTS coating is visible on the ZrP surface, which is consistent with XPS results, suggesting FOTS alone gives rise to a much thicker coating layer. The invisibility of FOTS on TEOS-coated ZrP indicates that a thinner layer of FOTS was deposited on the TEOS coating than it was on bare ZrP. This is because TEOS coating provides a surface with higher density of OH groups that the FOTS molecules with three reactive hydrolyzable groups can be grafted with, instead of self-polymerization, which has been reported in other studies.[20] Without the TEOS coating, the oligomeric FOTS, when attached to the ZrP surface, will yield a thick layer and be observed in SEM images.

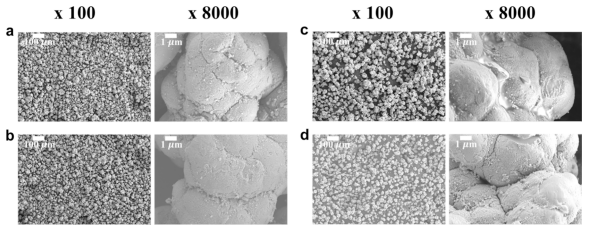

Figure 3. SEM images of uncoated ZrP (a), T (b), F12h (c), and TF12h (d) at 100× and 8000× magnification. "T" refers to ZrP coated with TEOS in liquid phase, while "F12h" represents ZrP coated with FOTS in vapor phase for 12 h. "TF12h" is ZrP coated with TEOS in liquid phase followed by FOTS in vapor phase for 12 h.

3.2. NH_4^+ and Ca^{2+} Binding Study. Figure 4a provides the results of an *in vitro* competitive ion study of uncoated and coated ZrP in a fixed amount of water solution containing 15 mM NH_4^+ and Ca^{2+}. Uncoated ZrP removes ~1.14 mequiv of NH_4^+/g of ZrP from the solution within the first 2 h of the study, but by 24 h the removal decreases somewhat to ~1.07 mequiv/g. In the meantime, Ca^{2+} removal by uncoated ZrP during 24 h is ~1.93 mequiv of Ca^{2+}/g of ZrP. The Ca^{2+} binding to the ZrP surface can replace adsorbed NH_4^+, which is released into the water solution, causing the decrease in NH_4^+ removal, since ZrP has a higher affinity for bivalent ions than monovalent ions.[5,12] All TVD-coated ZrPs have similar NH_4^+ equilibrium binding to uncoated ZrP. At equilibrium, they can remove ~1.2 mequiv NH_4^+/g, and there is no decline in NH_4^+ removal due to the coating's blockage of transfer of Ca^{2+}. However, TF12h (TEOS wet coating) and T24hF12h (TEOS TVD coating) are the only two materials that remove nearly zero Ca^{2+} from solution (0.05 and 0.14 meqiv/g, respectively), while TF1h, TF3h, and F12h all remove greater than 0.4 mequiv of Ca^{2+}/g of ZrP. This demonstrates the importance of TVD duration of FOTS coating and presence of TEOS coating. Longer TVD duration yields more complete surface coverage of the FOTS coating (verified by higher F concentration in XPS analysis above); thus, water with Ca^{2+} is less likely to penetrate the coating and reach the ZrP surface, leading to negligible removal of Ca^{2+} from solution. A TEOS coating, according to previous studies,[5,12] can provide abundant hydroxyl groups on the ZrP surface, which is the

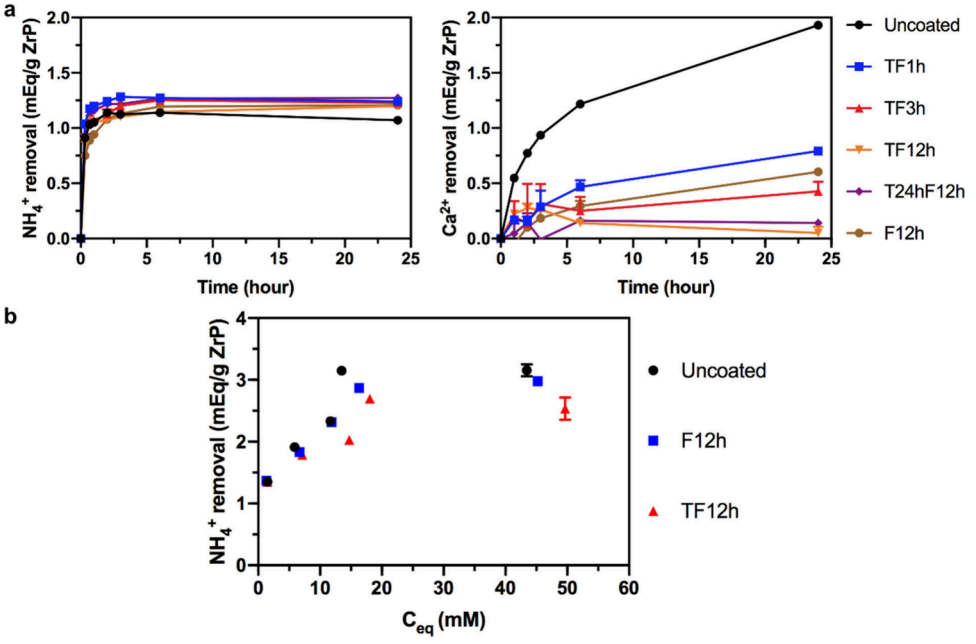

Figure 4. Competing ion binding study of uncoated and coated ZrP materials in a batch of water solution (15 mM NH_4^+, 15 mM Ca^{2+}, and 20 mM HEPES) (a) and equilibrium binding study of uncoated ZrP, F12h, and TF12h in stock solutions with a single ion (15/25/35/45/75 mM NH_4^+) (b). Each data point was determined based on at least 3 sampling experiments.

https://doi.org/10.1021/acs.langmuir.4c01877
Langmuir 2024, 40, 16502−16510

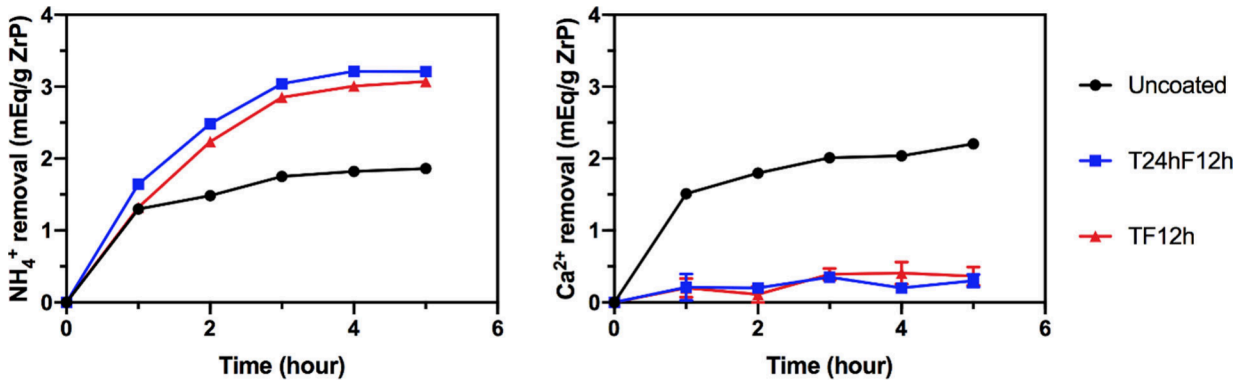

Figure 5. Competing ion binding study of uncoated and coated ZrP materials in a continuously replaced (every 20 min) water solution (14 mM NH_4^+, 12 mM Ca^{2+}). "TF12h" refers to ZrP coated with TEOS in liquid phase followed by FOTS in vapor phase for 12 h, while "T24hF12h" was ZrP coated by TEOS in vapor phase for 24 h followed by FOTS in vapor phase for 12 h.

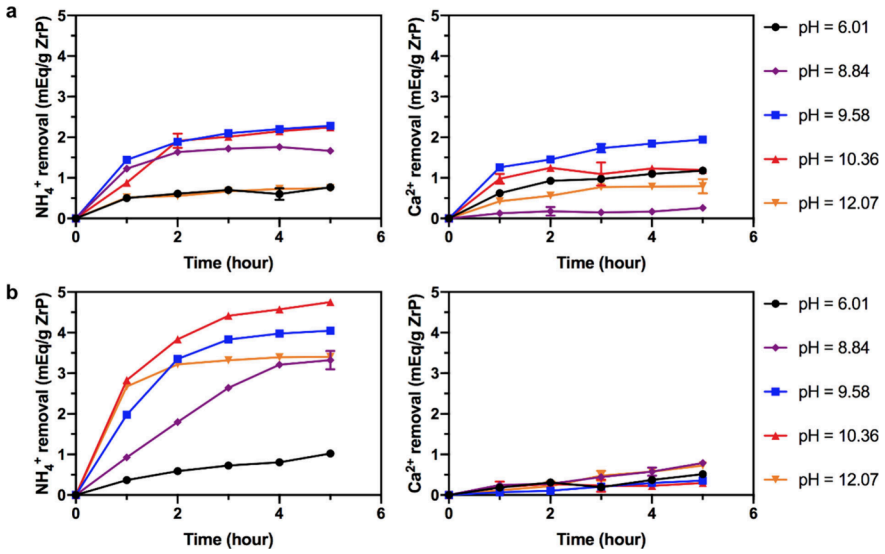

Figure 6. Competing ion binding study of uncoated ZrP (a) and T24hF12h (b) with hydrogen loading in a continuously replaced (every 20 min) water solution (14 mM NH_4^+, 12 mM Ca^{2+}, 0/3/7.6/14/28 mM NaOH).

key for a complete FOTS layer in the next coating step. For materials without a TEOS coating, such as F12h, water with Ca^{2+} is allowed by more coating defects to penetrate the FOTS layer even though F12h is prepared with a longer TVD duration, leading to a higher degree of Ca^{2+} binding. The effectiveness of T24hF12h on blocking Ca^{2+} indicates that TEOS can also be coated on the ZrP surface in the vapor phase.

Although Ca^{2+} adsorption on ZrP has been significantly reduced by the TVD coating, a higher NH_4^+ removal was not achieved in our competitive binding study. Thus, the ammonium binding capacity of ZrP was tested in solutions with different concentrations of a single ion (NH_4^+). Figure 4b presents the removal of NH_4^+ on uncoated and coated ZrP versus the equilibrium NH_4^+ concentration. The results indicate that the NH_4^+ removal by ZrP materials is proportional to the NH_4^+ concentration in stock solution. The uncoated ZrP can remove ~3.1 mequiv NH_4^+/g at an equilibrium concentration of ~15 mM, while F12h and TF12h remove respectively ~2.9 and ~2.7 mequiv NH_4^+/g at equilibrium. The slightly lower ammonium binding by coated materials implies that some binding sites are likely blocked by the gas-permeable and hydrophobic membrane from adsorption of NH_4^+. In addition, the increase in sodium concentration within the ZrP capsule due to a restraining effect of the membrane could also lower NH_4^+ removal, while for uncoated ZrP the sodium releases into stock solutions. On the other hand, F12h and TF12h have the same equilibrium binding, suggesting the effect of particulate surface area on binding capacity is insignificant, because gaseous NH_3 is highly diffusible.

Based on static binding studies shown in Figure 4, coated ZrP materials, i.e., TF12h and T24hF12h, have nearly zero Ca^{2+} binding, and their NH_4^+ removal is dependent on NH_4^+ concentrations in solution. In the next step, a binding study has been conducted in a more dynamic way where a water solution exposed to ZrP materials is replaced every 20 min to keep NH_4^+ and Ca^{2+} concentration relatively constant. This could also be considered as a simulated small intestine physiological condition of ESKD patients.[5] Figure 5 presents the results of this binding study. Uncoated ZrP cumulatively removes ~1.86 mequiv NH_4^+/g ZrP by 5 h; meanwhile TF12h and T24hF12h remove ~3.1 and ~3.2 mequiv NH_4^+/g ZrP, respectively. The improvement in the NH_4^+ binding capacity of coated materials is much more significant with this testing method, and the equilibrium NH_4^+ binding is consistent with that obtained

https://doi.org/10.1021/acs.langmuir.4c01877
Langmuir 2024, 40, 16502−16510

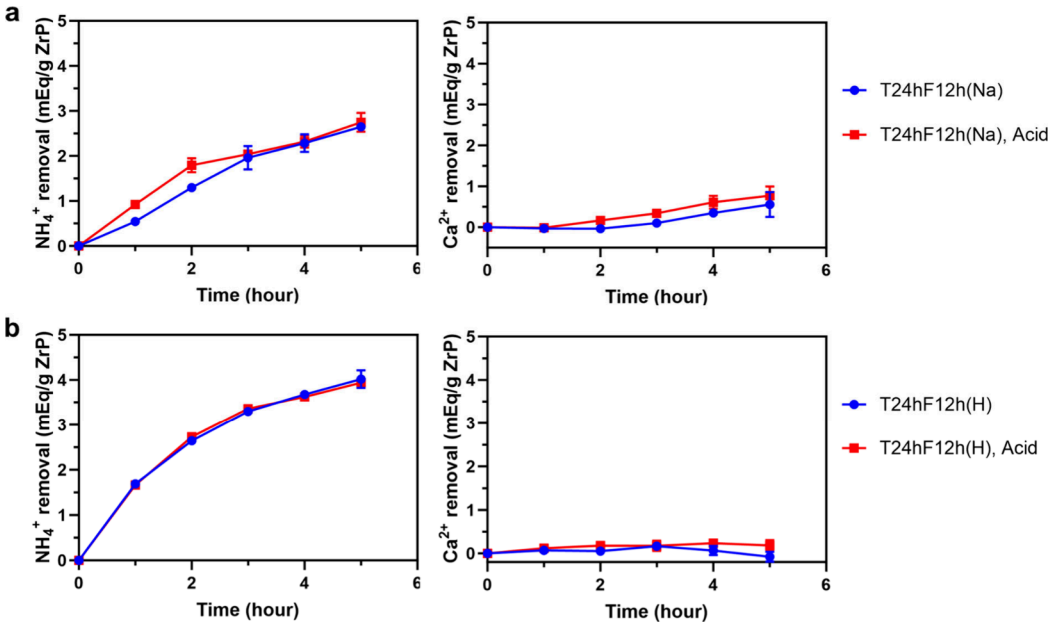

Figure 7. Competing ion binding study of Na-loaded (a) and H-loaded (b) ZrP with coating after acid exposure (solution pH is 5.9 for Na-loaded ZrP and 10.9 for H-loaded ZrP).

from the equilibrium binding study in Figure 4b. On the other hand, these two coated ZrP materials remove only ∼0.3 mequiv Ca^{2+}/g ZrP by 5 h, which is a huge improvement compared to ∼2.2 mequiv Ca^{2+}/g ZrP removed by uncoated ZrP. Therefore, ZrP with a gas-permeable and hydrophobic coating formed in the vapor phase has been demonstrated with excellent NH_4^+ binding selectivity and capacity.

The maximum NH_4^+ binding capacity achieved in equilibrium and the dynamic binding study has not reached the maximum indicated in binary binding studies (∼6 mequiv/g) for ZrP yet.[36−38] One reason is that our ZrP is partially Na-loaded, evidenced in the above XPS results where ∼5% sodium is present on the uncoated ZrP surface. ZrP total binding capacity could reach the maximum if ZrP is fully loaded with hydrogen because a lower pH within the ZrP capsule can facilitate the transfer of NH_3 across the membrane. The NaOH titration curves in Figure S1 show a pH of ∼7.3 for a Na-loaded ZrP solution and a pH of ∼3.8 for a H-loaded ZrP solution. With H-loaded ZrP, gaseous NH_3 can bind to the H^+, and NH_4^+ forms within the ZrP capsule, where the pH increases but not as much as with Na-loaded ZrP, which has internal accumulation of Na^+ and thus an increased pH.

3.3. Improved NH_4^+ Binding Capacity with H-Loaded ZrP. To find a sorbent with higher NH_4^+ binding capacity, we switched to study a H-loaded ZrP by applying the same coating condition (T24hF12h) and performing the binding study with continuously replacing the stock solution. Stock solutions with different concentrations of NaOH were prepared to investigate the effect of solution pH, which could influence the gradient of NH_3 across the membrane and thus the NH_4^+ concentration within the capsules and the resulting binding capacity. As a result, uncoated ZrP and T24hF12h both have a limited NH_4^+ removal (<∼1 mequiv/g) by 5 h with a solution pH of ∼6 (without NaOH addition), shown in Figure 6a,b, indicating acidic conditions in solution inhibits the amounts of NH_3 because NH_4^+ is in equilibrium with NH_3 and H^+ in any solution. With the addition of NaOH at concentrations of ∼3, ∼7.6, and ∼14 mM, uncoated ZrP can remove ∼2 mequiv NH_4^+/g by 5 h, and T24hF12h exhibits improved NH_4^+ binding capacities, which are above ∼3 mequiv/g. A NH_4^+ removal of 3.3 mequiv/g can be achieved at a pH of 8.84, which is close to the pH in the small bowel (pH ≈ 8) and dialysate from regeneration columns (pH = 8−9). In solution with pH values of 9.58 and 10.36 (∼7.6 and ∼14 mM NaOH), T24hF12h can remove ∼4 and 4.8 mequiv/g, respectively, by 5 h, showing the potential of H-loaded ZrP to achieve higher NH_4^+ binding compared to that (∼3.2 mequiv/g) from Na-loaded ZrP. Although these pH values are higher than realistic conditions, ZO-OH loaded with hydroxide can be added with sorbent materials to increase the gut pH to promote the NH_4^+ removal by coated ZrP.

The effect of solution pH on H-loaded ZrP ion exchange capacity has been reported previously.[36−44] In general, the ion binding capacity of ZrP can be improved by increasing the solution pH level. At higher pH, hydrogen ions released from ZrP can be neutralized by OH^- in solution, while in acidic solution with lower pH, the buildup of released hydrogen will lower the ion exchange capacity because hydrogen ion can also compete for ion sorption.[5,12] Here, the NaOH added in stock solution acts as a buffer to deplete H^+ in solution and release it from ZrP, such that the equilibrium $NH_4^+ \leftrightarrow NH_3 + H^+$ will shift to the right to have abundant amount of NH_3 to be removed by coated ZrPs. When the pH is raised to >12, the NH_4^+ binding capacity of T24hF12h during 5 h decreases to ∼3.4 mequiv/g because H^+ within the ZrP capsule and TVD coatings may diffuse to the stock solution given the higher pH gradient. Thus, the amount of H^+ remaining inside the ZrP capsule will become less for NH_3 to adsorb. In other words, the higher pH within the ZrP capsule leads to a lower NH_4^+ removal. The Ca^{2+} removal of T24hF12h is only ∼0.35 mequiv/g at a pH of 10.36, which is significantly lower than the removal (>1.1 mequiv/g) of uncoated ZrP. Thus, the NH_4^+ binding capacity and selectivity have been effectively improved by using H-loaded ZrP with TVD coatings.

3.4. Coating Resistance to Acid Exposures. The resistance of ZrP as an oral sorbent to acidic solution is

https://doi.org/10.1021/acs.langmuir.4c01877
Langmuir 2024, 40, 16502−16510

critical because it will pass through the stomach, which is a low-pH environment (pH = 2−3), before entering the small intestine. Figure S4 shows that there is no significant change for coated ZrP materials in SEM images, XPS atomic composition, and WCA after acid treatment. Figure 7a,b shows the results of the dynamic binding study on coated materials (a: Na-loaded T24hF12h in a solution of 14 mM NH_4^+ and 12 mM Ca^{2+}; b: H-loaded T24hF12h in a solution of 14 mM NH_4^+, 12 mM Ca^{2+}, and 14 mM NaOH) before and after acid treatment (pH = 2). The Na-loaded and H-loaded T24hF12h can remove respectively ∼2.8 and ∼4 mequiv NH_4^+/g in 5 h, which are not adversely impacted by the acid treatment. The lower NH_4^+ removal (∼4 mequiv/g) of H-loaded ZrP than that reported in the previous section (∼4.7 mequiv/g) is because of the slight difference in pH of stock solutions in the two binding studies (10.9 vs 10.36). As explained above, a pH too high in the stock solution could also decrease the NH_4^+ removal. On the other hand, the ability of acid-treated materials to remove Ca^{2+} does not change significantly (only ∼0.2 mequiv Ca^{2+}/g increase compared to results before acid treatment), which means that the NH_4^+ removal selectivity does not decline and that TVD coatings on the two ZrP materials remain intact in an acid environment. FOTS has been prominent with its chemical stability and inertness,[45] and it has three reactive groups and thus a high degree of cross-linking, which is more stable in acid exposure. The outstanding acid resistance of T24hF12h materials suggests that ZrP with the gas-permeable and hydrophobic membrane formed in the vapor phase is promising as an oral sorbent for ESKD patients.

4. CONCLUSION

This study has successfully developed a solventless coating protocol that effectively coats ZrP with TEOS and FOTS via vapor phase deposition, which significantly reduces the preparation length compared to the wet chemistry approach and eliminates the usage of solvents such as acetone. The TVD duration was optimized based on the coated materials' ability to selectively remove NH_4^+ in a static binding study. The dynamic *in vitro* binding study shows a maximum NH_4^+ binding capacity of ∼3.2 mequiv/g for Na-loaded ZrP, which can be further improved by replacing Na-loaded ZrP with H-loaded ZrP for TVD coatings (∼4.7 mequiv/g), and both coated materials barely remove Ca^{2+} in the meantime. FOTS-coated ZrP materials by TVD also exhibit excellent resistance in acid treatment. H-loaded ZrP is thus a suitable material for TEOS and FOTS coating by TVD, and the coated ZrP could serve as an oral sorbent to diminish BUN levels in patients with ESKD. It may also serve as a sorbent for NH_4^+ generated by urease in columns used for regeneration of dialysate. Moving forward, *in vitro* tests are needed to determine whether the coatings are solubilized in a water suspension or fouled or degraded by some biological components of the gut such as acid, protein, and bile salts. These studies will indicate whether it is reasonable to proceed to animal trials of this potentially valuable oral sorbent.

ASSOCIATED CONTENT

Supporting Information

The Supporting Information is available free of charge at https://pubs.acs.org/doi/10.1021/acs.langmuir.4c01877.

NaOH titration curve for Na-loaded and H-loaded ZrP; atomic surface composition, SEM images, and water contact angle of H-loaded and Na-loaded ZrP materials at different coating conditions before and after acid exposure (PDF)

AUTHOR INFORMATION

Corresponding Authors

Stephen R. Ash − *Nephrology Department, Indiana University Health Arnett Hospital, Lafayette, Indiana 47905, United States; CEO, HemoCleanse Technologies, LLC, Lafayette, Indiana 47904, United States*; Email: sash@hemocleanse.com

Lei Li − *Department of Chemical and Petroleum Engineering, University of Pittsburgh, Pittsburgh, Pennsylvania 15260, United States*; orcid.org/0000-0002-8679-9575; Email: lel55@pitt.edu

Authors

Yihan Song − *Department of Chemical and Petroleum Engineering, University of Pittsburgh, Pittsburgh, Pennsylvania 15260, United States*; orcid.org/0000-0001-6417-5174

Sang-Ho Ye − *McGowan Institute for Regenerative Medicine, Pittsburgh, Pennsylvania 15210, United States; Department of Surgery, University of Pittsburgh, Pittsburgh, Pennsylvania 15260, United States*

Complete contact information is available at: https://pubs.acs.org/10.1021/acs.langmuir.4c01877

Funding

This research was funded by HemoCleanse Technologies, LLC (Lafayette, IN, USA).

Notes

The authors declare no competing financial interest.

ACKNOWLEDGMENTS

We thank Dr. Haitao Liu for laboratory space and the use of the UV/vis spectrometer. Part of this work was conducted at the Molecular Analysis Facility, a National Nanotechnology Coordinated Infrastructure (NNCI) site at the University of Washington, which is supported in part by funds from the National Science Foundation (awards NNCI-2025489 and NNCI-1542101), the Molecular Engineering & Sciences Institute, and the Clean Energy Institute.

REFERENCES

(1) Kalantar-Zadeh, K.; Jafar, T. H.; Nitsch, D.; Neuen, B. L.; Perkovic, V. Chronic kidney disease. *Lancet* **2021**, *398* (10302), 786−802.

(2) De Nicola, L.; Zoccali, C. Chronic kidney disease prevalence in the general population: heterogeneity and concerns. *Nephrol Dial Transplant* **2016**, *31* (3), 331−5.

(3) Centers for Diease Control and Prevention. Chronic Kidney Disease Surveillance System website. https://nccd.cdc.gov/CKD (accessed June 20, 2023).

(4) van Gelder, M. K.; Jong, J. A. W.; Folkertsma, L.; Guo, Y.; Bluchel, C.; Verhaar, M. C.; Odijk, M.; Van Nostrum, C. F.; Hennink, W. E.; Gerritsen, K. G. F. Urea removal strategies for dialysate regeneration in a wearable artificial kidney. *Biomaterials* **2020**, *234*, No. 119735.

(5) Richards, E.; Ye, S. H.; Ash, S. R.; Li, L. Developing a Selective Zirconium Phosphate Cation Exchanger to Adsorb Ammonium:

Effect of a Gas-Permeable and Hydrophobic Coating. *Langmuir* **2022**, *38* (28), 8677−8685.
(6) Ramada, D. L.; de Vries, J.; Vollenbroek, J.; Noor, N.; Ter Beek, O.; Mihaila, S. M.; Wieringa, F.; Masereeuw, R.; Gerritsen, K.; Stamatialis, D. Portable, wearable and implantable artificial kidney systems: needs, opportunities and challenges. *Nat. Rev. Nephrol* **2023**, *19* (8), 481−490.
(7) Sinnakirouchenan, R.; Holley, J. L. Peritoneal dialysis versus hemodialysis: risks, benefits, and access issues. *Adv. Chronic Kidney Dis* **2011**, *18* (6), 428−32.
(8) Mujais, S.; Story, K. Peritoneal dialysis in the US: evaluation of outcomes in contemporary cohorts. *Kidney Int. Suppl* **2006**, *70* (103), 521−526.
(9) Zha, Y.; Qian, Q. Protein Nutrition and Malnutrition in CKD and ESRD. *Nutrients* **2017**, *9* (3), 208.
(10) Broers, N. J. H.; Martens, R. J. H.; Canaud, B.; Cornelis, T.; Dejagere, T.; Diederen, N. M. P.; Hermans, M. M. H.; Konings, C.; Stifft, F.; Wirtz, J.; Leunissen, K. M. L.; van der Sande, F. M.; Kooman, J. P. Health-related quality of life in end-stage renal disease patients: the effects of starting dialysis in the first year after the transition period. *Int. Urol Nephrol* **2018**, *50* (6), 1131−1142.
(11) Himmelfarb, J.; Ratner, B. Wearable artificial kidney: problems, progress and prospects. *Nat. Rev. Nephrol* **2020**, *16* (10), 558−559.
(12) Richards, E.; Ye, S. H.; Ash, S. R.; Li, L. A Perfluorocarbon-Coated ZrP Cation Exchanger with Excellent Ammonium Selectivity and Chemical Stability: An Oral Sorbent for End-Stage Kidney Disease (ESKD). *Langmuir* **2023**, *39* (22), 7912−7921.
(13) van Gelder, M. K.; Mihaila, S. M.; Jansen, J.; Wester, M.; Verhaar, M. C.; Joles, J. A.; Stamatialis, D.; Masereeuw, R.; Gerritsen, K. G. F. From portable dialysis to a bioengineered kidney. *Expert Rev. Med. Devices* **2018**, *15* (5), 323−336.
(14) Gura, V.; Rivara, M. B.; Bieber, S.; Munshi, R.; Smith, N. C.; Linke, L.; Kundzins, J.; Beizai, M.; Ezon, C.; Kessler, L.; Himmelfarb, J. A wearable artificial kidney for patients with end-stage renal disease. *JCI Insight* **2016**, *1* (8), 86397.
(15) Ash, S. R. Oral sorbents for small, charged uremic toxins, and carbon block for regeneration of dialysate: Fourth down and long. *Artif Organs* **2023**, *47* (1), 217−221.
(16) Chao, C. T.; Lin, S. H. Uremic Vascular Calcification: The Pathogenic Roles and Gastrointestinal Decontamination of Uremic Toxins. *Toxins (Basel)* **2020**, *12* (12), 812.
(17) Ash, S. R.; Singh, B.; Lavin, P. T.; Stavros, F.; Rasmussen, H. S. A phase 2 study on the treatment of hyperkalemia in patients with chronic kidney disease suggests that the selective potassium trap, ZS-9, is safe and efficient. *Kidney Int.* **2015**, *88* (2), 404−11.
(18) Fishbane, S.; Ford, M.; Fukagawa, M.; McCafferty, K.; Rastogi, A.; Spinowitz, B.; Staroselskiy, K.; Vishnevskiy, K.; Lisovskaja, V.; Al-Shurbaji, A.; Guzman, N.; Bhandari, S. A Phase 3b, Randomized, Double-Blind, Placebo-Controlled Study of Sodium Zirconium Cyclosilicate for Reducing the Incidence of Predialysis Hyperkalemia. *J. Am. Soc. Nephrol* **2019**, *30* (9), 1723−1733.
(19) Fadeev, A. Y.; McCarthy, T. J. Trialkylsilane Monolayers Covalently Attached to Silicon Surfaces: Wettability Studies Indicating that Molecular Topography Contributes to Contact Angle Hysteresis. *Langmuir* **1999**, *15* (11), 3759−3766.
(20) Fadeev, A. Y.; McCarthy, T. J. Self-Assembly Is Not the Only Reaction Possible between Alkyltrichlorosilanes and Surfaces: Monomolecular and Oligomeric Covalently Attached Layers of Dichloro- and Trichloroalkylsilanes on Silicon. *Langmuir* **2000**, *16* (18), 7268−7274.
(21) Genzer, J.; Efimenko, K.; Fischer, D. A. Molecular Orientation and Grafting Density in Semifluorinated Self-Assembled Monolayers of Mono-, Di-, and Trichloro Silanes on Silica Substrates. *Langmuir* **2002**, *18* (24), 9307−9311.
(22) Dong, J.; Wang, A.; Ng, K. S.; Mao, G. Self-assembly of octadecyltrichlorosilane monolayers on silicon-based substrates by chemical vapor deposition. *Thin Solid Films* **2006**, *515*, 2116−2122.
(23) Silverio, V.; Canane, P. A. G.; Cardoso, S. Surface wettability and stability of chemically modified silicon, glass and polymeric surfaces via room temperature chemical vapor deposition. *Colloids Surf., A* **2019**, *570*, 210−217.
(24) Song, X.; Zhai, J.; Wang, Y.; Jiang, L. Fabrication of Superhydrophobic Surfaces by Self-Assembly and Their Water-Adhesion Properties. *Langmuir* **2005**, *109*, 4048−4052.
(25) Li, L.; Li, B.; Dong, J.; Zhang, J. Roles of silanes and silicones in forming superhydrophobic and superoleophobic materials. *J. Mater. Chem. A* **2016**, *4* (36), 13677−13725.
(26) Nazarov, A.; Petrunin, M.; Maksaeva, L.; Yurasova, T.; Traverso, P.; Marshakov, A. Vapour Phase Deposition of Thin Siloxane Coatings on the Iron Surface. The Impact of the Layer Structure and Oxygen Adsorption on Corrosion Stability. *Coatings* **2021**, *11* (10), 1217.
(27) Zhang, F.; Chen, S.; Dong, L.; Lei, Y.; Liu, T.; Yin, Y. Preparation of superhydrophobic films on titanium as effective corrosion barriers. *Appl. Surf. Sci.* **2011**, *257* (7), 2587−2591.
(28) Rissanen, A.; Tappura, K.; Laamanen, M.; Puurunen, R.; Farm, E.; Ritala, M.; Leskela, M., Vapor-phase self-assembled monolayers for improved MEMS reliability. In *Sensors 2010*; IEEE, Waikoloa, HI, USA, 2010; pp 767−770.
(29) Zhuang, Y. X.; Hansen, O.; Knieling, T.; Wang, C.; Rombach, P.; Lang, W.; Benecke, W.; Kehlenbeck, M.; Koblitz, J. Vapor-Phase Self-Assembled Monolayers for Anti-Stiction Applications in MEMS. *J. Microelectromech. Syst.* **2007**, *16* (6), 1451−1460.
(30) Badv, M.; Jaffer, I. H.; Weitz, J. I.; Didar, T. F. An omniphobic lubricant-infused coating produced by chemical vapor deposition of hydrophobic organosilanes attenuates clotting on catheter surfaces. *Sci. Rep* **2017**, *7* (1), No. 11639.
(31) Hong, J. K.; Mathur, K.; Ruhoff, A. M.; Akhavan, B.; Waterhouse, A.; Neto, C. Design Optimization of Perfluorinated Liquid-Infused Surfaces for Blood-Contacting Applications. *Adv. Mater. Interfaces* **2022**, *9* (10), No. 2102214.
(32) Ahn, J. K.; Oh, S. J.; Park, H.; Song, Y.; Kwon, S. J.; Shin, H.-B. Vapor-phase deposition-based self-assembled monolayer for an electrochemical sensing platform. *AIP Advances* **2020**, *10* (4), No. 045213.
(33) Yuan, X.; Wolf, N.; Mayer, D.; Offenha Usser, A.; Wo Rdenweber, R. Vapor-Phase Deposition and Electronic Characterization of 3-Aminopropyltriethoxysilane Self-Assembled Monolayers on Silicon Dioxide. *Langmuir* **2019**, *35* (25), 8183−8190.
(34) Cooper, O.; Phan, H. P.; Wang, B.; Lowe, S.; Day, C. J.; Nguyen, N. T.; Tiralongo, J. Functional Microarray Platform with Self-Assembled Monolayers on 3C-Silicon Carbide. *Langmuir* **2020**, *36* (44), 13181−13192.
(35) Adamkiewicz, M.; O'Hara, T.; O'Hagan, D.; Hähner, G. A vapor phase deposition of self-assembled monolayers: Vinyl-terminated films of volatile silanes on silicon oxide substrates. *Thin Solid Films* **2012**, *520* (22), 6719−6723.
(36) Ash, S. R.; Carr, D. Oral sorbent for removing toxins of kidney failure combining anion and cation exchangers. U.S. Patent US10,668,098 B2, Jun. 2, 2020.
(37) Hasegawa, Y.; Aoki, H. The Ion-exchange Behavior of the Ammonium Ion on Crystalline Zirconium Phosphate. *Bull. Chem. Soc. Jpn.* **1973**, *46*, 836.
(38) Clearfield, A.; Hunter, R. A. On the mechanism of ion exchange in zirconium phosphate. XIV. The effect of crystallinity on NH4+/H+ exchange of α-zirconium phosphate. *J. Inorg. Nucl. Chem.* **1976**, *38*, 1085.
(39) Clearfield, A.; Duax, W. L.; Medina, A. S.; Smith, G. D.; Thomas, J. R. On the Mechanism of Ion Exchange in Crystalline Zirconium Phosphates. I. Sodium Ion Exchange of α-Zirconium Phosphate. *J. Phys. Chem.* **1969**, *73*, 3424−3430.
(40) Nancollas, G. H.; Pekarek, V. Sorption properties of zirconium phosphate of various crystallinities. *J. Inorg. Nucl. Chem.* **1965**, *27*, 1409−1418.
(41) Clearfield, A.; Stynes, J. A. The preparation of crystalline zirconium phosphate and some observations on its ion exchange behaviour. *J. Inorg. Nucl. Chem.* **1964**, *26*, 117−129.

https://doi.org/10.1021/acs.langmuir.4c01877
Langmuir 2024, 40, 16502−16510

(42) Pan, B.; Zhang, Q.; Du, W.; Zhang, W.; Pan, B.; Zhang, Q.; Xu, Z.; Zhang, Q. Selective heavy metals removal from waters by amorphous zirconium phosphate: behavior and mechanism. *Water Res.* **2007**, *41* (14), 3103−11.
(43) Jiang, P.; Pan, B.; Pan, B.; Zhang, W.; Zhang, Q. A comparative study on lead sorption by amorphous and crystalline zirconium phosphates. *Colloids Surf., A* **2008**, *322* (1−3), 108−112.
(44) Avdibegović, D.; Zhang, W.; Xu, J.; Regadío, M.; Koivula, R.; Binnemans, K. Selective ion-exchange separation of scandium(III) over iron(III) by crystalline α-zirconium phosphate platelets under acidic conditions. *Sep. Purif. Technol.* **2019**, *215*, 81−90.
(45) Jovicic, V.; Khan, M. J.; Zbogar-Rasic, A.; Fedorova, N.; Poser, A.; Swoboda, P.; Delgado, A. Degradation of Low Concentrated Perfluorinated Compounds (PFCs) from Water Samples Using Non-Thermal Atmospheric Plasma (NTAP). *Energies* **2018**, *11* (5), 1290.

https://doi.org/10.1021/acs.langmuir.4c01877
Langmuir 2024, 40, 16502−16510